energies

MDPI

Article

Combined Utilization of Cylinder and Different Shaped Alumina Nanoparticles in the Base Fluid for the Effective Cooling System Design of Lithium-Ion Battery Packs

Fatih Selimefendigil [1,2,*], Furkan Dilbaz [2] and Hakan F. Öztop [3,4]

[1] Department of Mechanical Engineering, College of Engineering, King Faisal University, Al Ahsa 31982, Saudi Arabia
[2] Department of Mechanical Engineering, Manisa Celal Bayar University, Manisa 45140, Turkey
[3] Department of Mechanical Engineering, Technology Faculty, Fırat University, Elazığ 23119, Turkey
[4] Department of Medical Research, China Medical University Hospital, China Medical University, Taichung 404327, Taiwan
* Correspondence: fgil@kfu.edu.sa

Abstract: It is important to consider the thermal management of lithium-ion batteries to overcome their limitations in usage and improve their performance and life cycles. In this study, a novel cooling system for the thermal management of lithium-ion battery packs is proposed by using an inner cylinder in the cooling channel and different-shaped nanoparticles in the base fluid, which is used as the cooling medium. The performance improvements in a 20 Ah capacity battery are compared by using a water–boehmite alumina (AlOOH) nanofluid, considering cylinder-, brick-, and blade-shaped nanoparticles up to a solid volume fraction of 2%. The numerical analysis is conducted using the finite element method, and Reynolds numbers between 100 and 600 are considered. When the efficacy of the coolants utilized is compared, it is apparent that as the Reynolds number increases, both cooling media decrease the highest temperature and homogenize the temperatures in the battery. The utilization of the cylinder in the mini-channel results in a 2 °C temperature drop at Re = 600 as compared to the flat channel. A boehmite alumina nanofluid with a 2% volume fraction reduces the maximum temperature by 5.1% at Re = 200. When the shape effect of the nanofluid is examined, it is noted that the cylinder-shaped particle improves the temperature by 4.93% as compared to blade-shaped nanoparticles and 7.32% as compared to brick-shaped nanoparticles. Thus, the combined utilization of a nanofluid containing cylindrical-shaped nanoparticles as the cooling medium and a cylinder in the mini-channel of a battery thermal management system provides an effective cooling system for the thermal management of the battery pack. The outcomes of this work are helpful for further system design and optimization studies related to battery thermal management.

Keywords: nanoparticle shape; cylinder; thermal management; lithium-ion battery pack; finite element method

Citation: Selimefendigil, F.; Dilbaz, F.; Öztop, H.F. Combined Utilization of Cylinder and Different Shaped Alumina Nanoparticles in the Base Fluid for the Effective Cooling System Design of Lithium-Ion Battery Packs. *Energies* **2023**, *16*, 3966. https://doi.org/10.3390/en16093966

Academic Editor: Fangming Jiang

Received: 23 March 2023
Revised: 4 May 2023
Accepted: 6 May 2023
Published: 8 May 2023

1. Introduction

The need for alternative energy sources is growing due to environmental concerns and increasing energy prices [1]. In this aspect, lithium-ion batteries (LIBs) are considered the ideal energy source that can be used instead of internal combustion engines due to their high specific energy and power density, as well as their long cycle life and status as a green energy source. However, a single lithium-ion battery cell does not have enough power and voltage to move a vehicle. Therefore, this technology is possible with battery packs (BPs), which are formed by connecting a large number of lithium-ion cells in series or parallel to obtain the required power and voltage [2]. Lithium-ion batteries have various thermal limitations, such as capacity/power fade, self-discharge, and thermal runaway [3]. In addition to these limitations, Li-ion batteries generate heat during the charge/discharge cycle, which leads to

an increase in the temperature of the unit cells. If the battery cell indicates performance at an operating temperature higher than the recommended operating temperature range, this may result in shortened battery life, damage to unit cells, and even the firing/explosion of the battery pack. Therefore, the thermal management of electrochemical products such as Li-ion batteries is vital [3,4]. Ensuring an appropriate operating temperature (20–50 °C) for lithium-ion batteries and uniform temperature distribution between battery cells are two essential factors for these products to perform at the desired efficiency [5,6]. There are two basic cooling methods to control the temperature generated during the charge/discharge cycle of batteries: active (air cooling and liquid cooling) and passive (PCM and heat pipe) [7]. Active methods require some external power input to achieve an advancement in the heat transfer rate [8]. The equipment required for this method increases the cost, weight, and complexity of the system. Passive methods generally intend to increase heat transfer by using techniques such as accommodating secondary structures in the flow, aiming to extend surfaces with addition fins, and providing surface roughness [8], while in the literature, many active and passive methods have been offered for different thermal engineering applications [9–18].

There are various studies related to thermal management in the literature to ensure the efficient operation of batteries. Deng et al. [19], to maintain effective cooling for prismatic lithium-ion batteries, designed a cooling plate with a serpentine channel in the shape of a U-tube. They examined many parameters, including the number of channels, their placement, and the fluid inlet temperature. As a result, they noted that the increase in the number of channels provides effective cooling, and the channel placement affects the thermal performance. Behi et al. [20] considered three dissimilar cooling methods for efficient cooling of an LTO (lithium-titanate-oxide) battery. As a result, the most effective one at high discharge was noted as the straight heat pipe-assisted technique. This method reduced the highest temperature on the LTO battery pack by 32.6% when compared to the air-cooling technique. Xie et al. [21] used two different vortex generators for the performance enhancement of pouch-type Li-ion batteries while numerical simulations were performed. It was observed that the vortex generators improved the performance. Wang et al. [22] explored the effects of the number of mini-channels and mass flow rate on the temperature distribution of the battery module by utilizing a single-factor analysis method. They noted that the cooling structure design had profound impacts on the peak temperature factor in the battery pack. They also observed that the peak temperature decreases as the mini-channel number in the cooling system (CS) increases. Chen et al. [23] compared different cooling techniques for battery thermal management systems. Power consumption, refrigerant, maximum temperature value, temperature difference in the battery pack (BP), and extra weight on the module were analyzed. It was noted that the air CS needed more energy to have the same average temperature. They also noted that fin CS added additional weight to the system compared to other methods. Lan et al. [24] designed a CS for batteries that accommodated mini duct tubes. In their study, cooling performance was examined for different discharge rates, different flow rates, and different tube systems. As a result, they noted that the system effectively reduced the maximum temperature that occurred on the battery cell and the temperature difference that took place. Zhao et al. [25] included a mini-channel liquid-cooled cylinder for cylindrical batteries. The impacts of the channel number, mass flow, and inlet size on the performance of the CS were explored. By using more than four channels, the temperature of the BP was kept within the optimum operating range.

The thermal performance of LiBs can be enhanced by introducing nanofluids into the liquid CS. Nanofluids are formed by dispersing nano-sized particles in the cooling fluid [26]. Nanofluids have a greater specific surface area compared to standard working conditions, and their transport properties can be adjusted by altering the particle composition, concentration, size, and shape [26]. Nanofluids outperform typical working conditions in heat management systems. Many aspects of nanofluids, including the shape effects of nanoparticles, using more than one particle in the base fluid (hybrid nanofluids), non-Newtonian nanofluids, and single and multi-phase approaches to modeling, have been considered in various thermal systems.

There are various studies in the literature on the effect of nanofluids as a cooling medium on the thermal performance of batteries. Kiani et al. [27] experimentally investigated the CS for pouch-type LiB modules. It was shown that the thermal efficiency of the system by using nanoparticles in the cooling medium increased significantly. Sefidan et al. [28] used a cylindrical Li-ion battery of type 18650 in a narrow cylindrical tank filled with alumina–water nanofluid, which was used as a cooling medium. The generated heat during discharge was transported to the nanofluid while it was dissipated from the tank surface by airflow. By using this technique, the maximum temperature was reduced by 16–24 K. Chen and Li [29] performed an efficient CS for lithium-ion batteries by using pulsing heat pipes. Various effects on the efficiency of the system, such as ambient temperature and working conditions, were analyzed. The working environment was compared to a nanofluid containing TiO_2 nanoparticles. It was reported that the PHP with TiO_2 nanofluid delivered more effective thermal performance.

The aim of this article is to investigate the nanoparticle shape effect in the thermal management of LiBs and to examine the effect of cooling plates, including channels with cylinders. Cooling channels with and without cylinders are compared in terms of their thermal performances on the BP. Then, the thermal performances of alumina–water nanofluids containing three different particle shapes (cylinder, brick, and blade) at different volume ratios (between 0% and 2%) are compared at different Reynolds numbers. In the literature, nanofluids have been used in the thermal management of BP systems, while the combined utilization of nanoparticle shape effects and a cooling plate with an inner cylinder has never been considered. As many aspects of nanofluids, including non-Newtonian fluid behavior, shape effects, utilization of hybrid particles in the base fluid, and many more, have been considered in the thermal management of different energy systems, this is the first work that uses nanoparticle shape effects and the installation of a cylinder in the mini-channel for the LiB thermal management system. As the CS design for LiB packs and installed systems is important for the efficient utilization of those devices and thermal management, the outcomes of the present work will be beneficial for further performance improvement and optimization studies.

2. Model Definition

The battery pack used in this study consists of three unit cells and a flow field. A unit cell consists of two battery cells and an aluminum cooling plate with dimensions of $100 \times 100 \times 2$ mm. In the CS, five U-type pipes of 1.5 mm diameter inside the cooling plate are utilized. The cooling is provided by passing the coolant through these pipes. In order to increase the thermal performance of the cooling plate, 0.5 mm diameter cylinders were added to these pipes. Figure 1a represents the unit cell of the BP, Figure 1b shows the BP, and Figure 1c shows a U-type channel with cylinders. The capacity of the prismatic battery is 20 Ampere-hour (Ah). In this work, the battery module with LiPF6 electrolyte in ethylene carbonate (EC): ethylmethyl carbonate (EMC) (3:7 by volume) for liquid electrolyte, the graphite electrode LixC6 mesocarbon microbeads (MCMB) for anode, and the lithium manganese oxide (LMO) electrode $LiMn_2O_4$ spinel for cathode are utilized. The numerical studies are carried out using a discharge current of 100 amps and a discharge period of 180 s.

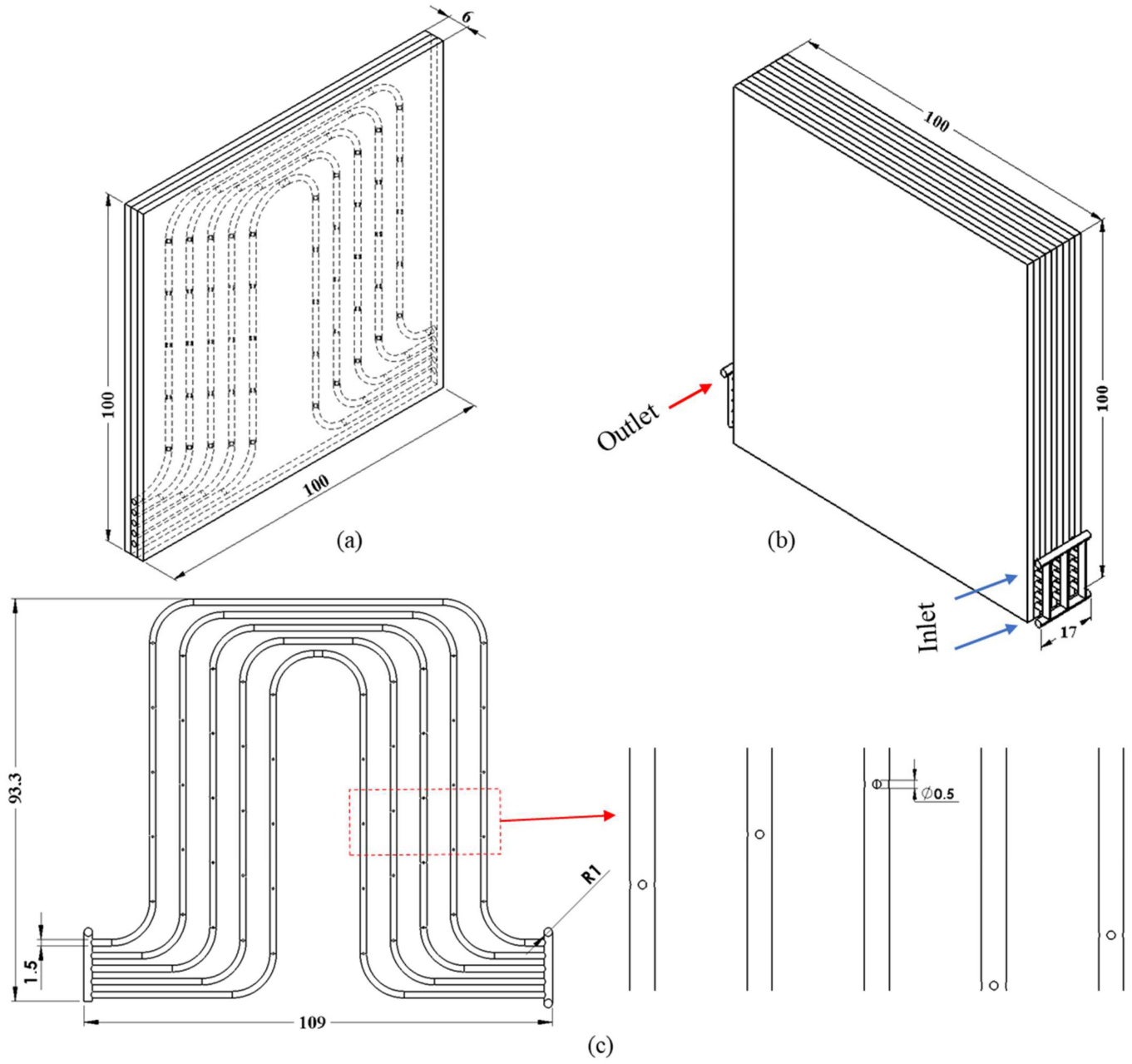

Figure 1. (**a**) Unit cell of the battery pack, (**b**) battery pack, and (**c**) U-type channel with cylinder.

2.1. Thermal Model

Heat is generated in the BM as a result of the electro-chemical thermal reaction, while the heat is dispersed by the cooling plate. The heat produced (HP) by a single battery cell is specified by using the energy conservation equation [30] as follows:

$$\frac{\partial}{\partial t}\left(\rho_b C_{p,b} T_b\right) = \nabla \cdot \left(k_b \nabla T_b\right) + \dot{Q}_{gen} \tag{1}$$

where $\dot{Q}_{gen}$(W) represents the HP, T_b(K) denotes the average temperature, ρ_b (kg·m^{-3}) represents the density across the cell, $C_{p,b}$ (J·kg^{-1}·K^{-1}) represents the specific heat capacity, and k_b (W·m^{-1}·K^{-1}) represents the thermal conductivity. Electrochemical processes and

cell internal resistance generate heat in a battery cell. The amount of heat created by the battery during discharge is defined as follows [30]:

$$\dot{Q}_{gen} = \dot{Q}_{ec} + \dot{Q}_j = \frac{1}{nF}(-T\Delta S) + I(E - V) \quad (2)$$

where ΔS indicates the entropy change, F indicates the Faraday's constant, n indicates the number of electrons in the electrochemical reactions, I represents the current that travels through the battery, V denotes the battery's operating voltage, and E denotes the open circuit voltage. The thermal conductivity of the battery is improved by assuming an anisotropic thermal conductivity [30]. The thermal conductivity calculations for a single cell based on the directions (x, y, and z) are as follows [30]:

$$k_{T,x} = \frac{\sum L_i * k_{T,i}}{\sum L_i} \quad (3)$$

$$k_{T,y} = \frac{\sum L_i}{\sum L_i / k_{T,i}} \quad (4)$$

$$k_{T,z} = \frac{\sum L_i * k_{T,i}}{\sum L_i} \quad (5)$$

where L_i is the thickness of a single cell's layer in a specific direction and $k_{T,i}$ denotes the thermal conductivities of the layers in that direction. The density and specific heat of a single cell are calculated as follows based on the qualities of the materials utilized [30]:

$$\rho_b = \frac{\sum L_i * \rho_i}{\sum L_i} \quad (6)$$

$$c_{p,b} = \frac{\sum L_i * c_{pi}}{\sum L_i} \quad (7)$$

The exterior walls of the BP are subjected to a convective boundary condition. The following is the heat emitted from the BP to the medium q_a ($W{\cdot}m^{-2}$), as calculated using Newton's cooling law:

$$q_a = h_a(T_{bm} - T_a) \quad (8)$$

where T_{bm} is the average temperature and T_a denotes the ambient temperature. Furthermore, the heat transfer coefficient h_a is assumed to be 5 ($W{\cdot}m^{-2}{\cdot}K^{-1}$). For the fluid moving through the pipes in the heat sink, the conservation equations are [30]:

$$\rho_w c_w \frac{\partial T_w}{\partial t} + \nabla\cdot\left(\rho_w c_w \vec{v} T_w\right) = \nabla\cdot(k_w \nabla T_w) \quad (9)$$

$$\nabla\cdot\vec{v} = 0 \quad (10)$$

$$\rho_w\left[\frac{\partial\vec{v}}{\partial t} + \left(\vec{v}\cdot\nabla\right)\vec{v}\right] = -\nabla P + \mu\nabla^2\vec{v} \quad (11)$$

The density of the fluid flowing through the coolant plate ($kg{\cdot}m^{-3}$), the specific heat capacity ($J{\cdot}kg^{-1}{\cdot}K^{-1}$), the thermal conductivity ($W{\cdot}m^{-1}{\cdot}K^{-1}$), the temperature (K), and the velocity ($m{\cdot}s^{-1}$) are indicated by ρ_w, c_w, k_w, T_w and $\vec{v}$, respectively.

2.2. Nanofluid Model

The nanofluid used in this study was obtained by adding nano-sized boehmite alumina particles in different shapes (brick, cylinder, blade) to water, which is the base fluid. Table 1 lists the thermophysical properties of the base fluid and the nanoparticles.

Table 1. Boehmite alumina nanoparticles and base fluid thermophysical properties [31].

Thermophysical Properties	ρ (kg·m^{-3})	C_p (J·kg^{-1}·K^{-1})	k (W·m^{-1}·K^{-1})	μ (Pa·s)
Boehmite Alumina (AlOOH)	3050	618.3	30	N/A
Water	996	4178	0.615	7.98×10^{-4}

The thermophysical properties of nanofluids using different nanoparticle shapes can be calculated with the following formulations: Equations (12) and (13) are used to calculate the density and specific heat of nanofluids for all particle forms, respectively [32]:

$$\rho_{nf} = \rho_f(1-\varphi) + \rho_{np}\varphi \tag{12}$$

$$(c_p)_{nf} = \frac{(1-\varphi)(\rho c_p)_f + \varphi(\rho c_p)_{np}}{\rho_{nf}} \tag{13}$$

The subscripts *nf*, *np*, and *f* denote the nanofluid, nanoparticle, and base fluid, respectively, and the nanofluid concentration is denoted by φ. Equations (14) and (15) are used to calculate the thermal conductivity and viscosities of nanofluids with cylinder-, brick-, and blade-shaped nano-sized particles [33,34]:

$$\frac{k_{nf}}{k_f} = 1 + \left(C_k^{shape} + C_k^{surface}\right)\varphi = 1 + C_k\varphi \tag{14}$$

$$\mu_{nf} = \mu_f\left(1 + A_1 + A_2\varphi^2\right) \tag{15}$$

where C_k^{shape} denotes the influence of the nanoparticle shape on the thermal conductivity and $C_k^{surface}$ represents the surface resistance impacted by the solid/liquid interface, which has a negative impact on nanofluid thermal conductivity. Table 2 lists the values of C_k for various nanoparticle geometries [34]. Table 3 also includes constants A1 and A2 for various particle shapes [34].

Table 2. For estimating the thermal conductivity of a dispersion comprising various particle geometries, the parameters used in Equation (14) and the aspect ratio of various particle forms are used [34].

Nanoparticles	Aspect Ratio	C_k	C_k^{shape}	$C_k^{surface} = C_k - C_k^{shape}$
Cylinder	1:8	3.95	4.82	−0.87
Brick	1:1:1	3.37	3.72	−0.35
Blade	1:6:1/12	2.74	8.26	−5.52

Table 3. The coefficients used to calculate the viscosity of dispersions with varying particle geometries [34].

Constants	Cylinder	Brick	Blade
$\mathbf{A_1}$	13.5	1.9	14.6
$\mathbf{A_2}$	904.4	471.4	123.3

2.3. Numerical Method

The efficiency of the CS built for the thermal management of the LiB, as well as the efficiency of the nanofluid shape effect on temperature, are investigated in the present study using the Comsol Multiphysics 5.5 software package. In the simulations, first the electrochemistry of the battery cell is solved utilizing a 1D cell model, and then the HP in the battery module and temperature profiles are predicted utilizing a 3D model. In

the Comsol Multiphysics 5.5 program, the laminar flow and heat transfer features are integrated with the non-isothermal flow subsystem, and the average heat generation value is obtained as in Ref. [35]. The battery pack density is 2055.2 ($kg \cdot m^{-3}$), the specific heat capacity is 1399.1 ($J \cdot kg^{-1} \cdot K^{-1}$), and its thermal conductivity is diagonal (x: 29.55, y: 0.89724, z: 29.55 ($W \cdot m^{-1} \cdot K^{-1}$)).

Boundary Conditions

During the simulations, the discharge operated in the battery is assumed to be 180 s constant and 5C. In addition, the cooling medium is regarded as having a fully developed laminar flow. The volumetric flow is applied in the inlet zone of the intended model, while the atmospheric boundary condition in the outlet zone is preserved. A convective boundary condition is applied to the outer walls of the battery pack, and the heat transfer coefficient is assumed to be 5 ($W \cdot m^{-2} \cdot K^{-1}$). Here, the ambient temperature is taken as 30 °C. This temperature value is the same for the battery cells, cooling plate, and fluid inlet temperature. Moreover, the contact resistance and radiation effects between the battery and the cooling plate can be neglected. For the inner walls of the channels, no-slip boundary conditions are imposed. Furthermore, for the fluid flowing through the channels, Reynolds numbers ranging from 100 to 600 are considered.

2.4. Mesh Independence

In computational fluid dynamics, the outcomes can vary according to the number of grids and their quality. The grid independence investigation on a battery pack was carried out utilizing a cooling plate with channels and cylinders at a Reynolds number of 200 and a constant discharge rate of 5C. In the battery model, which is built by the combination of 3 unit cells, 5 solution meshes varying between 3,809,799 and 11,852,718 elements were generated, and the average skewness quality of these grid structures was 0.6585. Figure 2 shows that the greatest temperature value changes based on the mesh number. A total of 11 million elements seemed to be sufficient for this examination. The grid structure on the battery pack is shown in Figure 3. Figure 4 depicts the mesh structure's quality in terms of geometry.

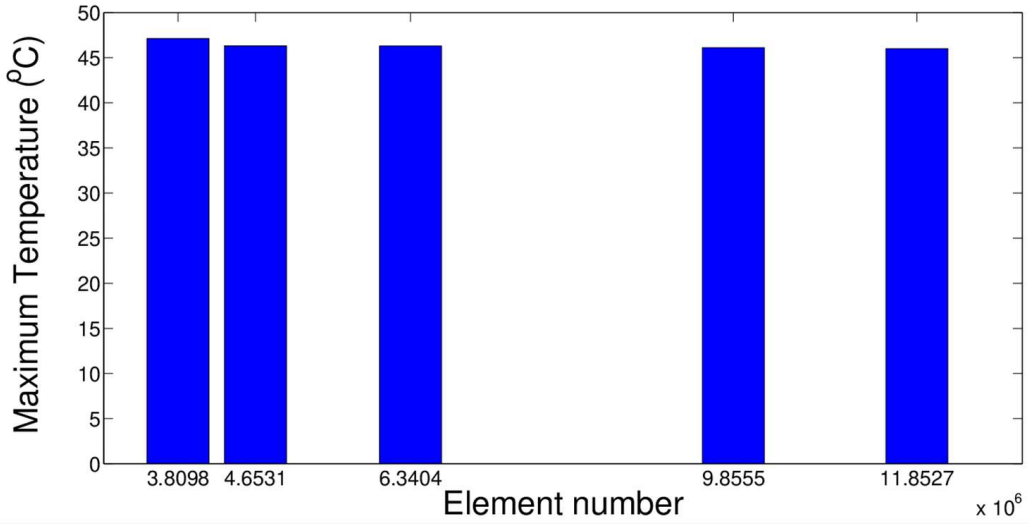

Figure 2. Grid independence for battery model.

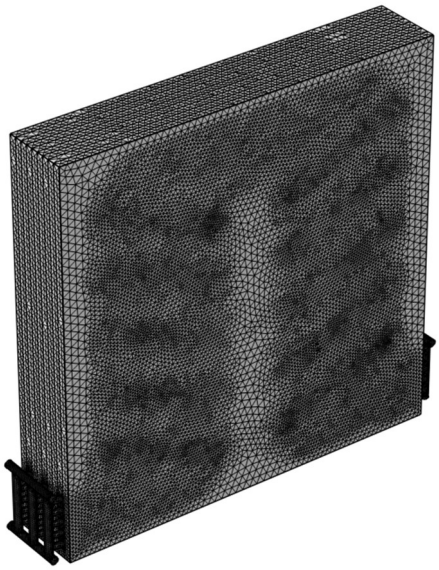

Figure 3. The grid structure on the battery model.

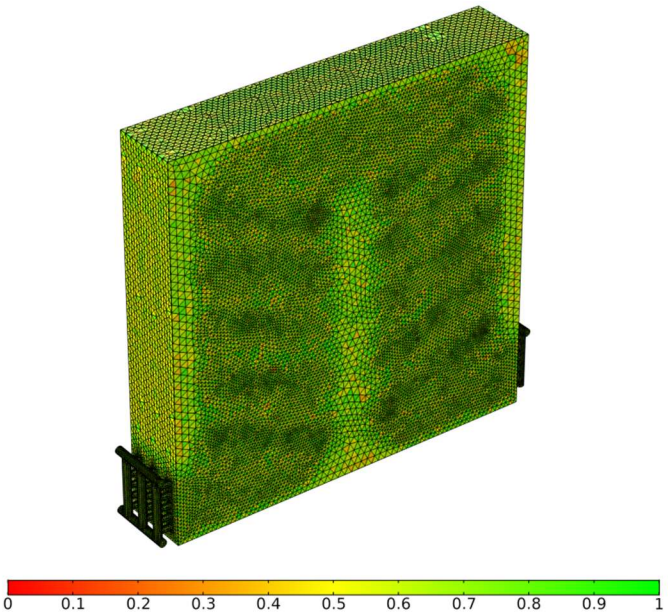

Figure 4. Quality of the mesh generated on the battery.

2.5. Code Validation

The validity of the code utilized for the results' reliability is evaluated by referring to the work of Siruvuri and Budarapu [35]. They utilized the symmetry condition to evaluate the thermal efficiency of a cooling system designed for a 1.5 Ah battery pack at a constant discharge rate and a discharge current of 90 A. With an environment and entrance temperature of 37 °C, they utilized a fully developed laminar flow boundary condition. A comparison of maximum temperature versus different flow rates is given in Figure 5a. At the lowest flow rate, the discrepancy is 9.04%, while in other cases the deviation is below 2%. In another validation test, the effects of using a cylinder on the convective heat transfer in a differentially heated cavity are explored, as in the study available in Roslan et al. [36]. In the work, different nanoparticles were used for further thermal performance enhancement, while the impacts of cylinder rotation and size were also examined. Figure 5b shows the comparison of the average Nusselt number for two different cylinder sizes (R = 0 and R = 0.4) by using Cu–water

nanofluid at 5% nanoparticle loading. The deviations between the results are 4% without the cylinder and 4.6% with the cylinder.

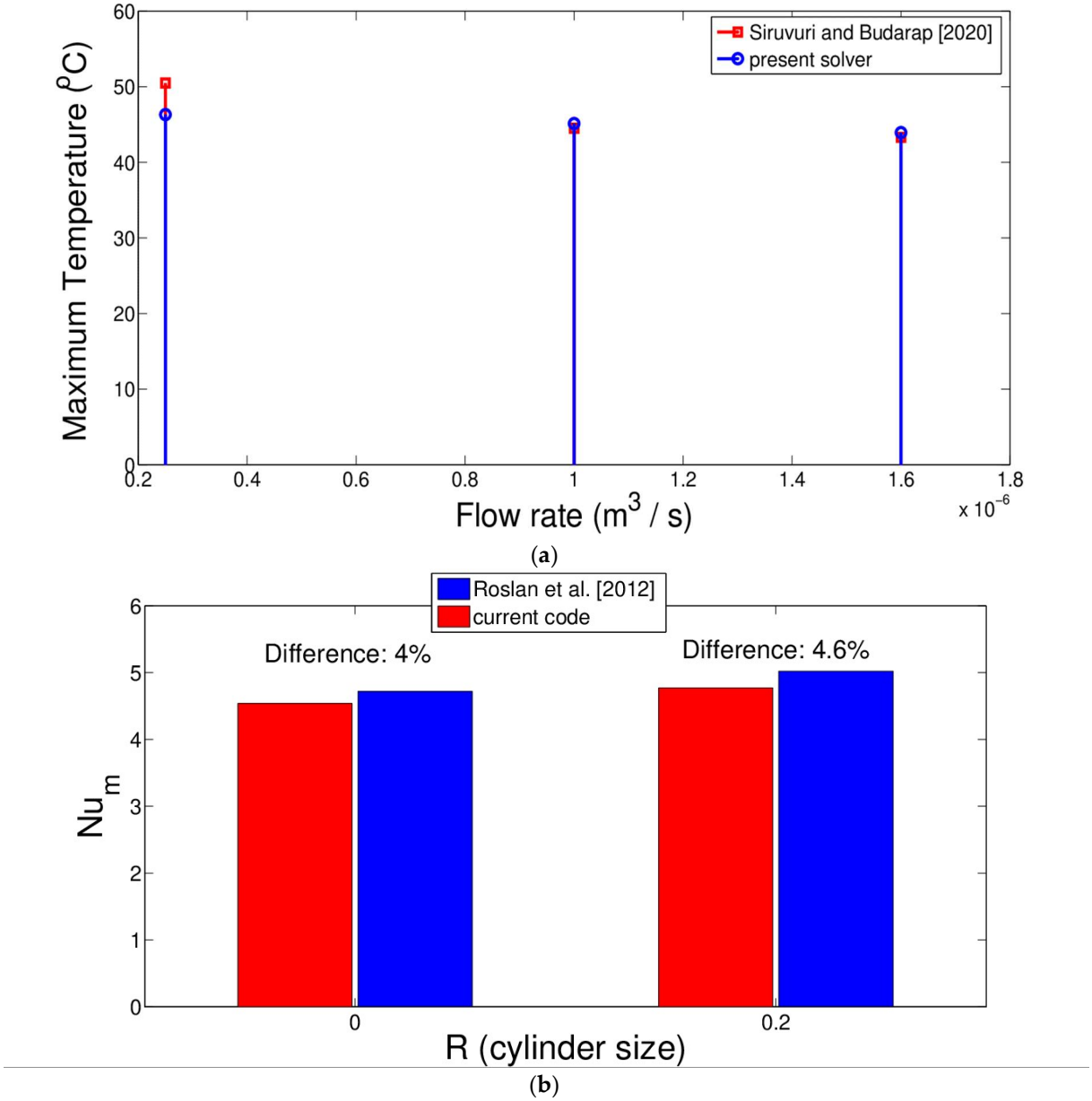

Figure 5. Confirmation test based on battery thermal management, as in the results of Siruvuri and Budarapu [35], where maximum temperature is given for different flow rates (**a**). Average Nu comparisons at two different cylinder sizes for the study analyzing the effects of using cylinders on convective heat transfer with Cu–water nanofluid at 5% solid volume fraction are available in Roslan et al. [36] (**b**). (**a**) Results of Siruvuri and Budarapu [35]. (**b**) Results of Roslan et al. [36].

3. Results and Discussion

This section compares the thermal efficiency of a cooling plate with cylinder-containing mini-channels designed for LiB thermal management against a flat-tube cooling plate. Furthermore, the effect of nanoparticle loading on the thermal management of batteries is explored at various volume ratios and Re.

At four different Re, the effect of cooling plates in the mini-channel with or without cylinders on coil temperature is explored. Cylinders with a diameter of 0.5 mm are added to the mini-channels on the cooling plate. Simulations are carried out for the case where

the cooling medium is a boehmite alumina (AlOOH) nanofluid at a constant discharge rate of 5C, an inlet temperature of 30 °C, and a 2% nanoparticle loading in the base fluid of the cooling medium. Figure 6 shows the effect of the cylinders added to the mini-channels on the maximum temperature formed in the battery. As the Re value increases, the influence of the cooling plate of the mini-channels with cylinders on the maximum temperature in the battery becomes more prominent. It is noted that, at Re values of 100 and 600, the maximum temperature is further reduced by 0.5 and 2 °C, respectively, compared to the mini-channels without cylinders on the cooling plate. This is attributed to the increase in local velocity in the channel caused by the insertion of the cylinders, while thermal transport is enhanced. This is effective at higher fluid inlet velocities, and the findings of this investigation show that adding cylinders inside the mini-channels has positive impacts on cooling effectiveness and overall thermal performance improvements.

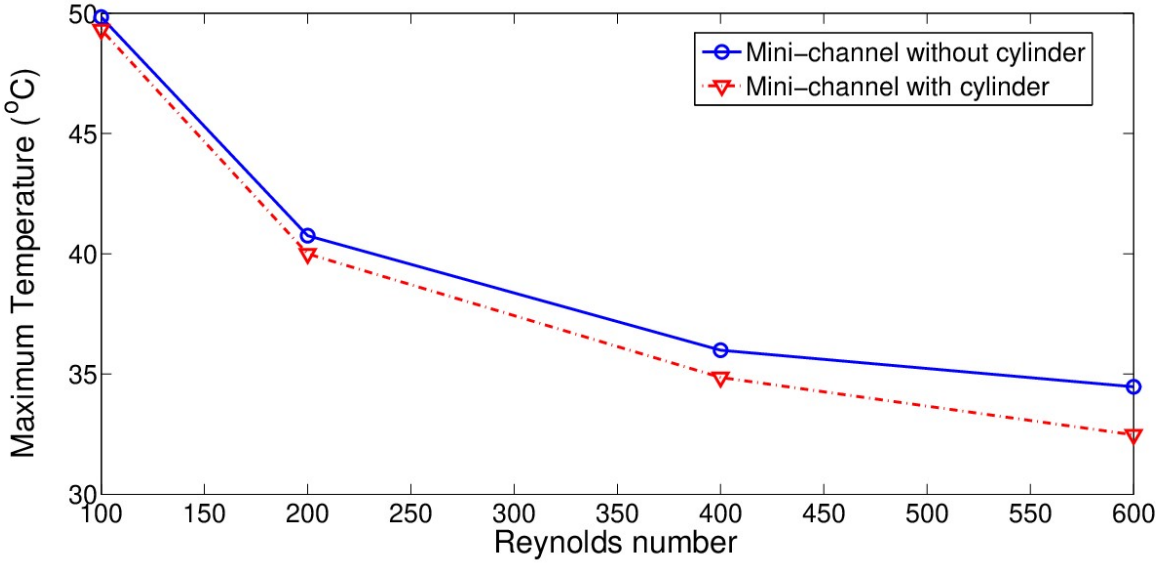

Figure 6. The effect of with-cylinder and without-cylinder mini-channels on the maximum temperature of the battery.

In this part, the influence of two distinct coolants (water and boehmite alumina nanofluid) flowing through the mini-channel with cylinder on the battery's thermal performance is explored at four different Re. The simulations are carried out at a constant discharge rate of 5C and an inlet temperature of 30 °C. For the efficient operation of the LiBs, they must perform in an ideal operating temperature range (20–50 °C) [5,6]. The effect of temperature on the battery pack with increasing Re of the cooling medium is shown in Figure 7, while its impact on the maximum temperature is presented in Table 4.

Table 4. Effect of cooling medium on maximum temperature.

Reynolds Number	Water	Nanofluid
	Max Temperature (°C)	Max Temperature (°C)
100	58.983	55.106
200	46.105	43.748
400	38.707	37.472
600	36.148	35.292

The heat absorption capability of the fluid flowing through the pipe increases as the value of Re rises. Thus, it keeps the battery pack from overheating and maintains a consistent temperature distribution. As a result, the battery's life is extended by limiting the occurrence of thermal runaways. The homogenization of the temperature distribution

on the BP is a necessary factor for these energy storage devices to work efficiently. It has been observed that a more uniform temperature distribution is achieved on the battery pack as the Re is increased.

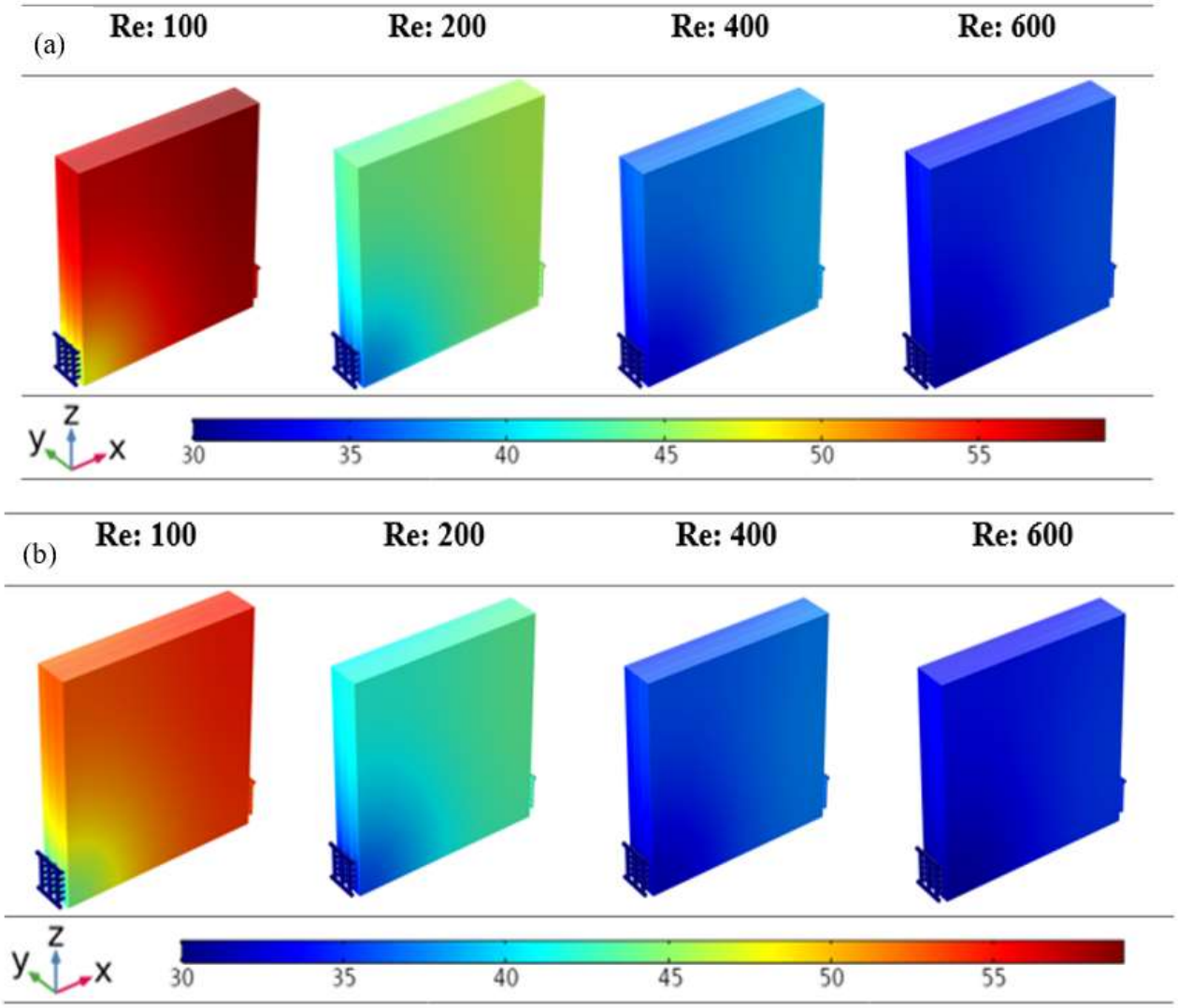

Figure 7. Effects of the cooling environment on the temperature distribution on the battery module: (**a**) effect of water on the temperature distribution on the battery pack; (**b**) effect of boehmite alumina (AlOOH) nanofluid, which has a 1% volume fraction and a cylindrical particle shape, on the temperature distribution on the battery pack.

It is observed that the highest temperature measurement in the BP decreased with increasing Re, which is due to the higher thermal transport and increased cooling effectiveness with higher fluid velocity. The highest temperature produced in the battery is observed when Re is equal to 100 in both cooling media. In this operating case, the temperature value is greater than the ideal operating temperature. However, when the Re number increases, the maximum temperature in the battery drops below 50 °C. Boehmite alumina (AlOOH) nanoparticles are added to the cooling medium to enhance the thermal performance of the battery, so that the maximum temperature is further reduced by 3.87, 2.357, 1.235, and 0.856 °C when the Re number is equal to 100, 200, 400, and 600, respectively. As a result, it clearly shows the effect of the cooling environment on the thermal performance of the BP.

Brick-, blade-, and cylindrical-shaped particles are loaded in the base fluid while the simulations are performed at 5C constant discharge rate, 2% volume ratio, and Re = 200.

Figure 8 shows the impact of increasing Re and different particle shapes on the temperature in the battery. While Re remains constant, the amount of nanofluid velocity is mostly determined by its viscosity [23]. The nanofluid with cylindrical particles has a higher viscosity at a constant volume ratio than the nanofluid with spherical solid particles. As a result, the nanofluid including cylindrical-shaped solid particles has high viscosity, resulting in faster velocities as compared to the nanofluid including brick- and blade-shaped solid particles. The heat transfer rate is also affected by using different-shaped particles [23]. For the reasons stated above, the most effective cooling is obtained when the particle shape is cylindrical. Similar trends were observed when convective heat transfer performance was explored in different studies available in the literature by using different-shaped nanoparticles. Bahiraei and Monavari [33] analyzed the impacts of nanoparticle shape on the thermohydraulic performance of nanofluids in the microplate heat exchanger, and their findings confirm the results presented here. Additionally, Nguyen et al. [37] indicated that greater heat transfer amounts were observed for platelet, cylinder, and brick particles. Vanaki et al. [38] showed that the highest heat transfer rates in the channel considering different-shaped nanoparticles were obtained by using platelet-, cylinder-, and blade-shaped solid particles. As it is shown in Figure 8, a temperature drop of 8.9 °C is achieved when using cylindrical-shaped nanoparticles in water at Re = 100, while this value is 5.2 °C for blade-shaped and 3.3 °C for brick-shaped nanoparticles in water. As the value of Re is increased, there is only a 2 °C drop in maximum temperature at Re = 600 by using cylindrical-shaped nanoparticles. The potential of using different-shaped nanoparticles for thermal performance improvement is higher for lower values of Re.

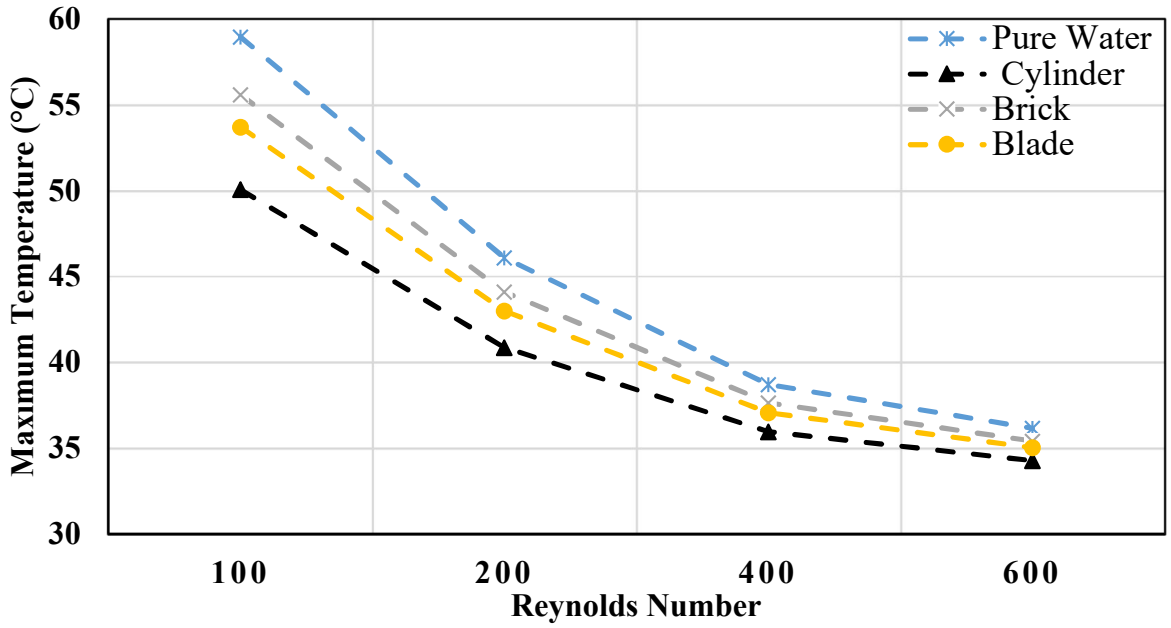

Figure 8. Impact of nanoparticle shape on battery temperature.

Figure 9 depicts the influence of the shape effect of a 2% volume ratio boehmite alumina nanofluid on the temperature difference in the BP. For the batteries to function properly, the temperature difference should be lower. The temperature difference is lowest when the solid nanoparticle shape is a cylinder, followed by the blade-shaped nanoparticle. The temperature difference drops from 10.6 °C to 9.7 °C when using cylindrical-shaped particles instead of pure water at Re = 100, while it drops from 4.64 °C to 3.30 °C at Re = 600.

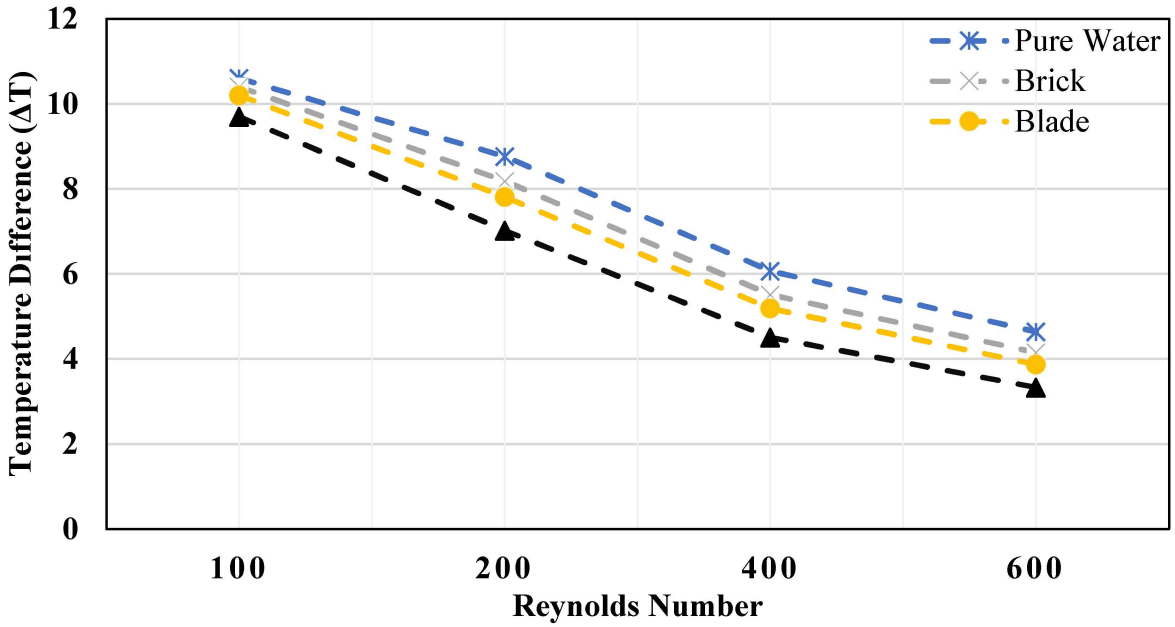

Figure 9. The influence of the geometry of a nanofluid with a volume fraction of 2% boehmite alumina on temperature differences in a battery.

In Figure 10, the influence of boehmite alumina nanofluid shape using a brick, blade, and cylinder with a solid volume fraction of 2% on the temperature distribution is seen at Re = 200. A battery with a homogenous temperature distribution not only improves efficiency and longevity, but it also decreases the possibility of thermal leakage. When cylinder-shaped nanoparticles are utilized, the temperature transition on the battery is slower and more uniform. Furthermore, the battery's maximum and minimum temperature range is lower than that of other nanoparticle forms.

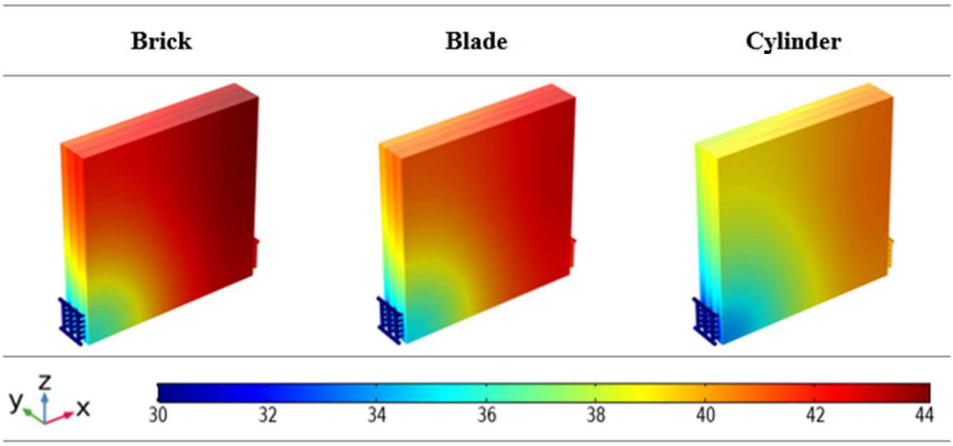

Figure 10. Shape effect of nanofluid on the temperature distribution of the battery.

The influence of cylindrical boehmite alumina (AlOOH) nanoparticles in the base fluid on the thermal efficiency of the cooling environment is explored in this part. Four different (0%, 0.5%, 1%, and 2%) solid particle volume fractions are used for this purpose, and simulations are performed at Re = 400. The impact of the solid volume fraction in the base fluid (water) on the temperature distribution on the battery module is demonstrated in Figure 11. The highest and lowest temperature values in the battery pack become closer to each other as the cylindrical-shaped nanoparticle loading amount increases. This results in a reduction in the temperature difference in the battery pack. Furthermore, it is seen that

increasing the solid volume fraction has a positive impact on the temperature distribution in the battery.

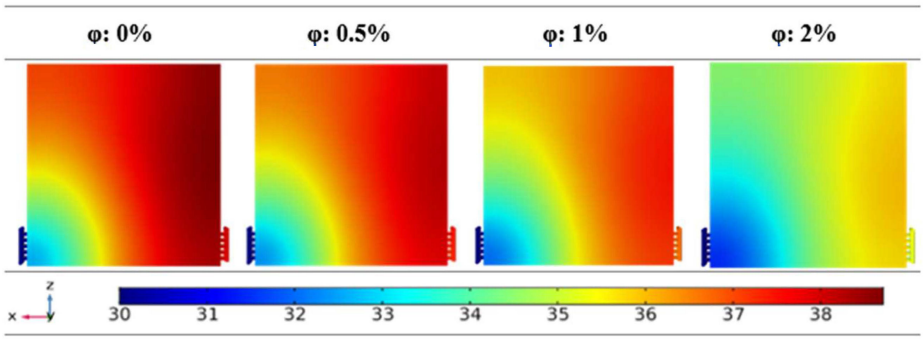

Figure 11. The influence of solid particle ratio on temperature dissipation on a battery module at Re = 400.

4. Conclusions

In this paper, a novel cooling system design for a battery with a capacity of 20 Ah is proposed by combining the utilization of inner cylinders in the cooling channels with different-shaped nanoparticles in the base fluid, which is used as the cooling medium. The important findings can be summarized as:

- It is observed that inserting cylinders into the channels has an influence on thermal performance, especially at higher values of Re. At Re = 600, the maximum temperature is reduced by 2 °C by using the cylinder in the channels of the CS.
- As the value of Re increases, the temperature of the BP decreases. Moreover, the incorporation of boehmite alumina nanoparticles into the base fluid enhances and accelerates the heat absorption of the cooling medium. It is observed that the case where the cooling medium is utilized as boehmite alumina (AlOOH) nanofluid performs better than the case where the coolant is water.
- When the effects of nanofluid shape on battery thermal performance are explored, cylindrical-shaped particles have better thermal efficiency as compared to solid particles in the shape of bricks and blades.
- When various shapes of solid particles in the nanofluid are compared at Re = 200 and a solid volume fraction of 2%, the cylinder-shaped particle outperforms the blade- and brick-shaped nanoparticles over the highest temperature by 4.93% and 7.32%, respectively.
- By using the cylinder-shaped nanoparticles and increasing the nanoparticle loading amount in the base fluid, more uniform temperature distributions are achieved.
- When the number of solid nanoparticles in the base fluid increases, the temperature difference in the BP decreases. The largest improvement is achieved at a solid volume fraction of 2%, where a maximum-temperature enhancement of 7.2% is achieved compared to the pure water case.

The present work can be extended to include an exergy analysis and a cost analysis of using nanofluids and different base fluids. The stability and performance degradation of using nanofluids after some time can be considered a future extension of the present work. As significant progress has been made in the field of material science, which may be applicable to the thermal management of the batteries [39–42], future studies should consider all relevant aspects, including material selection, operating conditions, and geometric factors, for the development of efficient battery cooling systems. Different nanoparticle types and channel configurations can be considered, which will increase the applicability of the present work towards the development of thermal management systems for BPs.

Author Contributions: Conceptualization, F.D. and F.S.; methodology, F.D. and F.S.; formal analysis, F.S., F.D. and H.F.Ö.; investigation, F.D. and F.S.; resources, F.D. and F.S.; data curation, F.S., F.D.

and H.F.Ö.; writing—original draft preparation, F.S. and F.D.; writing—review and editing, F.S., F.D. and H.F.Ö.; visualization, F.D. and F.S.; supervision, F.S. All authors have read and agreed to the published version of the manuscript.

Funding: This work was supported by the Deanship of Scientific Research, Vice Presidency for Graduate Studies and Scientific Research, King Faisal University, Saudi Arabia [Grant No. 2914].

Institutional Review Board Statement: Not applicable.

Informed Consent Statement: Not applicable.

Data Availability Statement: Not applicable.

Conflicts of Interest: The authors declare no conflict of interest.

Nomenclature

c_p	specific heat capacity
F	Faraday's constant
h	heat transfer coefficient
$\boldsymbol{I}$	current
k	thermal conductivity
L	length
p	pressure
Q_g	heat generation
S	entropy
T	temperature
t	time
q	heat flux
$\vec{v}$	velocity vector
V	voltage
x,y,z	x,y,z-coordinate
Greek letters	
ρ	density
μ	dynamic viscosity
φ	solid volume fraction
Subscripts	
a	ambient
bf	base fluid
nf	nanofluid
max	maximum
min	minimum
Abbreviations	
BP	battery pack
CS	cooling system
HP	heat produced
LIB	lithium-ion battery

References

1. Kiani, M.; Ansari, M.; Arshadi, A.A.; Houshfar, E.; Ashjaee, M. Hybrid thermal management of lithium-ion batteries using nanofluid, metal foam, and phase change material: An integrated numerical–experimental approach. *J. Therm. Anal. Calorim.* **2020**, *141*, 1703–1715. [CrossRef]
2. Fathabadi, H. High thermal performance lithium-ion battery pack including hybrid active–passive thermal management system for using in hybrid/electric vehicles. *Energy* **2014**, *70*, 529–538. [CrossRef]
3. Ismail, N.H.F.; Toha, S.F.; Azubir, N.A.M.; Ishak, N.H.M.; Hassan, I.D.M.K.; Ibrahim, B.S.K. Simplified heat generation model for lithium ion battery used in electric vehicle. *IOP Conf. Ser. Mater. Sci. Eng.* **2013**, *53*, 012014. [CrossRef]
4. Ma, S.; Jiang, M.; Tao, P.; Song, C.; Wu, J.; Wang, J.; Deng, T.; Shang, W. Temperature effect and thermal impact in lithium-ion batteries: A review. *Prog. Nat. Sci.* **2018**, *28*, 653–666. [CrossRef]
5. Wu, W.; Yang, X.; Zhang, G.; Chen, K.; Wang, S. Experimental investigation on the thermal performance of heat pipe-assisted phase change material based battery thermal management system. *Energy Convers. Manag.* **2017**, *138*, 486–492. [CrossRef]

6. Ren, Y.; Yu, Z.; Song, G. Thermal management of a Li-ion battery pack employing water evaporation. *J. Power Sources* **2017**, *360*, 166–171. [CrossRef]
7. Kaabinejadian, A.; Ahmadi, H.A.; Moghimi, M. Investigation of porous media effects on lithium-ion battery thermal management. *J. Therm. Anal. Calorim.* **2020**, *141*, 1619–1633. [CrossRef]
8. Saha, S.K.; Ranjan, H.; Emani, M.S.; Bharti, A.K. *Performance Evaluation Criteria in Heat Transfer Enhancement*; Springer International Publishing: Cham, Switzerland, 2020.
9. Moradikazerouni, A. Heat transfer characteristics of thermal energy storage system using single and multi-phase cooled heat sinks: A review. *J. Energy Storage* **2022**, *49*, 104097. [CrossRef]
10. Khalid, S.U.; Ali, H.M.; Nasir, M.A.; Pasha, R.A.; Said, Z.; Sundar, L.S.; Hussein, A.K. Experimental investigation of thermal performance characteristics of sintered copper wicked and grooved heat pipes: A comparative study. *J. Central South Univ.* **2021**, *28*, 3507–3520. [CrossRef]
11. Selimefendigil, F.; Öztop, H.F. Thermal management for conjugate heat transfer of curved solid conductive panel coupled with different cooling systems using non-Newtonian power law nanofluid applicable to photovoltaic panel systems. *Int. J. Therm. Sci.* **2022**, *173*, 107390. [CrossRef]
12. Moradikazerouni, A. Experimental and numerical investigation of traveling wave tube radial heat sink connector thermal stress and deformation with a focus on energy cost management. *Int. Commun. Heat Mass Transf.* **2022**, *131*, 105770. [CrossRef]
13. Hadi, F.; Ali, H.M. Experimental thermal and hydraulic study of super hydrophobic wavy mini channel heat sink using aqueous nanofluids. *Chem. Eng. Commun.* **2021**, *210*, 999–1021. [CrossRef]
14. Selimefendigil, F.; Öztop, H.F. Thermal management and performance improvement by using coupled effects of magnetic field and phase change material for hybrid nanoliquid convection through a 3D vented cylindrical cavity. *Int. J. Heat Mass Transf.* **2022**, *183*, 122233. [CrossRef]
15. Habib, H.M.; Ali, H.M.; Usman, M. Investigation of Condensate Retention on Horizontal Pin-Fin Tubes Using Water-Propanol Mixture. *Sustainability* **2022**, *14*, 835. [CrossRef]
16. Jafarimoghaddam, A.; Aberoumand, H.; Aberoumand, S.; Arani, A.A.A.; Habibollahzade, A. MHD wedge flow of nanofluids with an analytic solution to an especial case by Lambert W-function and Homotopy Perturbation Method. *Eng. Sci. Technol. Int. J.* **2017**, *20*, 1515–1530. [CrossRef]
17. Selimefendigil, F.; Öztop, H.F. Impacts of using an elastic fin on the phase change process under magnetic field during hybrid nanoliquid convection through a PCM-packed bed system. *Int. J. Mech. Sci.* **2022**, *216*, 106958. [CrossRef]
18. Hadi, F.; Ali, H.M.; Siddique, F. Hydrothermal performance evaluation of super hydrophobic square pin fin mini channel heat sink. *Therm. Sci.* **2022**, *26*, 3627–3640. [CrossRef]
19. Deng, T.; Zhang, G.; Ran, Y. Study on thermal management of rectangular Li-ion battery with serpentine-channel cold plate. *Int. J. Heat Mass Transf.* **2018**, *125*, 143–152. [CrossRef]
20. Behi, H.; Karimi, D.; Behi, M.; Jaguemont, J.; Ghanbarpour, M.; Behnia, M.; Berecibar, M.; Van Mierlo, J. Thermal management analysis using heat pipe in the high current discharging of lithium-ion battery in electric vehicles. *J. Energy Storage* **2020**, *32*, 101893. [CrossRef]
21. Xie, J.; Xie, Y.; Yuan, C. Numerical study of heat transfer enhancement using vortex generator for thermal management of lithium ion battery. *Int. J. Heat Mass Transf.* **2019**, *129*, 1184–1193. [CrossRef]
22. Wang, J.; Lu, S.; Wang, Y.; Li, C.; Wang, K. Effect analysis on thermal behavior enhancement of lithium–ion battery pack with different cooling structures. *J. Energy Storage* **2020**, *32*, 101800. [CrossRef]
23. Chen, D.; Jiang, J.; Kim, G.-H.; Yang, C.; Pesaran, A. Comparison of different cooling methods for lithium ion battery cells. *Appl. Therm. Eng.* **2016**, *94*, 846–854. [CrossRef]
24. Lan, C.; Xu, J.; Qiao, Y.; Ma, Y. Thermal management for high power lithium-ion battery by minichannel aluminum tubes. *Appl. Therm. Eng.* **2016**, *101*, 284–292. [CrossRef]
25. Zhao, J.; Rao, Z.; Li, Y. Thermal performance of mini-channel liquid cooled cylinder based battery thermal management for cylindrical lithium-ion power battery. *Energy Convers. Manag.* **2015**, *103*, 157–165. [CrossRef]
26. Bianco, V.; Manca, O.; Nardini, S.; Vafai, K. (Eds.) *Heat Transfer Enhancement with Nanofluids*; CRC Press: Boca Raton, FL, USA, 2015.
27. Kiani, M.; Omiddezyani, S.; Houshfar, E.; Miremadi, S.R.; Ashjaee, M.; Nejad, A.M. Lithium-ion battery thermal management system with Al_2O_3/AgO/CuO nanofluids and phase change material. *Appl. Therm. Eng.* **2020**, *180*, 115840. [CrossRef]
28. Sefidan, A.M.; Sojoudi, A.; Saha, S.C. Nanofluid-based cooling of cylindrical lithium-ion battery packs employing forced air flow. *Int. J. Therm. Sci.* **2017**, *117*, 44–58. [CrossRef]
29. Chen, M.; Li, J. Nanofluid-based pulsating heat pipe for thermal management of lithium-ion batteries for electric vehicles. *J. Energy Storage* **2020**, *32*, 101715. [CrossRef]
30. Monika, K.; Chakraborty, C.; Roy, S.; Dinda, S.; Singh, S.A.; Datta, S.P. Parametric investigation to optimize the thermal management of pouch type lithium-ion batteries with mini-channel cold plates. *Int. J. Heat Mass Transf.* **2021**, *164*, 120568. [CrossRef]
31. Mahian, O.; Kianifar, A.; Heris, S.Z.; Wongwises, S. First and second laws analysis of a minichannel-based solar collector using boehmite alumina nanofluids: Effects of nanoparticle shape and tube materials. *Int. J. Heat Mass Transf.* **2014**, *78*, 1166–1176. [CrossRef]

32. Alsarraf, J.; Moradikazerouni, A.; Shahsavar, A.; Afrand, M.; Salehipour, H.; Tran, M.D. Hydrothermal analysis of turbulent boehmite alumina nanofluid flow with different nanoparticle shapes in a minichannel heat exchanger using two-phase mixture model. *Phys. A Stat. Mech. Its Appl.* **2019**, *520*, 275–288. [CrossRef]
33. Bahiraei, M.; Monavari, A. Thermohydraulic characteristics of a micro plate heat exchanger operated with nanofluid considering different nanoparticle shapes. *Appl. Therm. Eng.* **2020**, *179*, 115621. [CrossRef]
34. Timofeeva, E.V.; Routbort, J.L.; Singh, D. Particle shape effects on thermophysical properties of alumina nanofluids. *J. Appl. Phys.* **2009**, *106*, 014304. [CrossRef]
35. Siruvuri, S.V.; Budarapu, P. Studies on thermal management of Lithium-ion battery pack using water as the cooling fluid. *J. Energy Storage* **2020**, *29*, 101377. [CrossRef]
36. Roslan, R.; Saleh, H.; Hashim, I. Effect of rotating cylinder on heat transfer in a square enclosure filled with nanofluids. *Int. J. Heat Mass Transf.* **2012**, *55*, 7247–7256. [CrossRef]
37. Nguyen, T.K.; Saidizad, A.; Jafaryar, M.; Sheikholeslami, M.; Gerdroodbary, M.B.; Moradi, R.; Shafee, A.; Li, Z. Influence of various shapes of CuO nanomaterial on nanofluid forced convection within a sinusoidal channel with obstacles. *Chem. Eng. Res. Des.* **2019**, *146*, 478–485. [CrossRef]
38. Vanaki, S.; Mohammed, H.; Abdollahi, A.; Wahid, M. Effect of nanoparticle shapes on the heat transfer enhancement in a wavy channel with different phase shifts. *J. Mol. Liq.* **2014**, *196*, 32–42. [CrossRef]
39. Song, H.; Kang, F. Recent Progress on Thermal Conduction of Graphene. *Acta Phys. Chim. Sin.* **2022**, *38*, 2101013. [CrossRef]
40. Han, S.Y.; Yue, B.H.; Yan, L.M. Research progress in the development of high-temperature proton exchange membranes based on phosphonic acid group. *Acta Phys. Chim. Sin.* **2014**, *30*, 8–21.
41. Younes, H.; Mao, M.; Murshed, S.S.; Lou, D.; Hong, H.; Peterson, G. Nanofluids: Key parameters to enhance thermal conductivity and its applications. *Appl. Therm. Eng.* **2022**, *207*, 118202. [CrossRef]
42. Younes, H.; Christensen, G.; Li, D.; Hong, H.; Ghaferi, A.A. Thermal conductivity of nanofluids. *J. Nanofluids* **2015**, *4*, 107–132. [CrossRef]